

Article

Doxorubicin Loaded PLGA Nanoparticle with Cationic/Anionic Polyelectrolyte Decoration: Characterization, and Its Therapeutic Potency

Li-Hui Tsai ¹, Chia-Hsiang Yen ¹, Hao-Ying Hsieh ^{1,2} and Tai-Horng Young ^{1,3,*}

¹ Department of Biomedical Engineering, National Taiwan University, Taipei 100, Taiwan; d07528009@ntu.edu.tw (L.-H.T.); f04548042@ntu.edu.tw (C.-H.Y.); Haoying@ntu.edu.tw (H.-Y.H.)

² Department of Dentistry, National Taiwan University Hospital, Taipei 100, Taiwan

³ Department of Biomedical Engineering, National Taiwan University Hospital, Taipei 100, Taiwan

* Correspondence: thyoung@ntu.edu.tw; Tel.: +886-2-2312-3456 (ext. 81455); Fax: +886-2-2394-0049

Abstract: Optimized Doxorubicin hydrochloride (DOX) loaded poly(lactic-co-glycolic acid) (PLGA) nanoparticles (DPN) were prepared by controlling the water/oil distribution of DOX at different pH solutions and controlling the electrostatic interaction between DOX and different terminated-end PLGAs. Furthermore, cationic polyethylenimine (PEI) and anionic poly(acrylic acid) (PAA) were alternately deposited on DPN surface to form PEI-DPN (IDPN) and PAA-PEI-DPN (AIDPN) to enhance cancer therapy potency. Compared to DPN, IDPN exhibited a slower release rate in physiological conditions but PEI was demonstrated to increase the efficiency of cellular uptake and endo/lysosomal escape ability. AIDPN, with the outermost negatively charged PAA layer, still retained better endo/lysosomal escape ability compared to DPN. In addition, AIDPN exhibited the best pH-dependent release profile with 1.6 times higher drug release in pH 5.5 than in pH 7.4. Therefore, AIDPN with the characteristics of PEI and PAA simultaneously was the most optional cancer therapy choice within these three PLGA nanoparticles. As the proposed nanoparticles integrated optimal procedure factors, and possessed cationic and anionic outlayer, our drug delivery nanoparticles can provide an alternative solution to current drug delivery technologies.

Keywords: doxorubicin; carboxylic acid terminated PLGA; ester terminated PLGA; polyethylenimine; poly(acrylic acid); endo/lysosomal escape; pH-dependent



Citation: Tsai, L.-H.; Yen, C.-H.; Hsieh, H.-Y.; Young, T.-H. Doxorubicin Loaded PLGA Nanoparticle with Cationic/Anionic Polyelectrolyte Decoration: Characterization, and Its Therapeutic Potency. *Polymers* **2021**, *13*, 693. <https://doi.org/10.3390/polym13050693>

Academic Editor: Iolanda De Marco

Received: 10 February 2021

Accepted: 21 February 2021

Published: 25 February 2021

Publisher's Note: MDPI stays neutral with regard to jurisdictional claims in published maps and institutional affiliations.



Copyright: © 2021 by the authors. Licensee MDPI, Basel, Switzerland. This article is an open access article distributed under the terms and conditions of the Creative Commons Attribution (CC BY) license (<https://creativecommons.org/licenses/by/4.0/>).

1. Introduction

Nanomedicine [1] plays an important role in cancer therapy because it can accumulate in tumors with a high vessel density, surrounded by an enhanced permeability and retention (EPR) effect [2,3]. Compared to the fast elimination of free drugs, nanomedicine exhibits a sustained release of up to four weeks [4,5]. Recently, many materials have been used to make drug delivery nanoparticles [6]. These materials should demonstrate biocompatibility, biodegradability, and low toxicity [7,8]. Poly(lactic-co-glycolic acid) (PLGA) is one of the most successful polymers used in the drug delivery system and is approved by the Food and Drug Administration (FDA) and the European Medicines Agency (EMA) in drug delivery systems [9,10]. Depending on the properties of drugs, preparation methods such as emulsification–evaporation, nanoprecipitation, spontaneous emulsion solvent diffusion, and membrane emulsification, have been chosen to produce drug-loaded PLGA nanoparticles [11,12].

Doxorubicin hydrochloride (DOX), an anthracycline anticancer drug, is used widely in several human cancers by DNA damage through two proposed mechanisms, which are topoisomerase II inhibition and free radical generation [13,14]. However, dose-limited cardiotoxicity and myelosuppression restrict DOX treatment in cancer therapy [15,16]. Antitumor drugs encapsulated in biodegradable polymers is one of the successful methods used to reduce their side effects [17,18].

The purpose of this study is to systematically analyze and optimize the effect of various variables on the size, zeta potential, and encapsulated efficiency percentage (EE%) of drug-loaded PLGA nanoparticles. In general, PLGA nanoparticles are deficient in the endo/lysosomes escape capability. Therefore, polyethylenimine (PEI), with the “proton sponge” effect rupture endo/lysosomes [19–22] was employed in the system by direct addition of PEI to nanoparticle formulation and by coating on PLGA nanoparticle surface. However, the positive charge of PEI is potentially cytotoxic and is tended to aggregate with serum protein [23,24]. To diminish this defect of PEI, another anionic polyelectrolyte poly(acrylic acid) (PAA) was involved in this drug-loaded nanomedicine, which could be adsorbed on PEI because of its anionic polyelectrolyte property [25].

In the present study, DOX-loaded PLGA nanoparticle (DPN), PEI-DPN (IDPN), and PAA-PEI-DPN (AIDPN) were prepared. Characterization of these nanoparticles, including particle size, zeta potential, morphology on transmission electron microscopy (TEM), and DOX release profile were determined. Cell cytotoxicity, cellular uptake, and endo/lysosomes escape of DPN, IDPN, and AIDPN were analyzed using A549, non-small cell lung cancer (NSCLC) cell line. A549 was chosen as the cell testing model because lung cancer is the leading cancer-related cause of death, and NSCLC is the most common type of lung cancer [26,27]. Finally, nanoparticles decorated with the combination of cationic/anionic polyelectrolyte (PEI/PAA) were found to be the most suitable in cancer therapy.

2. Materials and Methods

2.1. Materials

PLGA (carboxylic acid terminated, $M_w = 7000$ – $17,000$ Da; ester terminated, $M_w = 30,000$ – $60,000$ Da), polyvinyl alcohol (PVA, $M_w = 13,000$ – $23,000$ Da), dichloromethane (DCM), polyethylenimine (PEI, $M_w = 25,000$ Da), poly(acrylic acid) (PAA, $M_w = 15,000$ Da), dimethyl sulfoxide (DMSO), and 3-(4,5-dimethylthiazol-2-yl)-2,5-diphenyltetrazolium bromide (MTT) were purchased from Sigma-Aldrich (St. Louis, MO, USA). Doxorubicin hydrochloride (DOX) was purchased from LC Laboratories (Woburn, MA, USA). Ultrapure water (18.2 M Ω ·cm at 25 °C) was prepared by Cascada Purification System (Washington, NY, USA).

2.2. Preparation of DOX Loaded PLGA Nanoparticles

DOX-loaded PLGA nanoparticles were prepared using the double emulsion (W1/O/W2) method. Briefly, 0.5% DOX aqueous solution (W1) was added to 2% carboxylic acid terminated PLGA (A-PLGA) or ester terminated PLGA (E-PLGA) in DCM (oil phase; O) with a 1:5 volume ratio and sonicated in 80% amplitude for 60 s to emulsify W1-in-O (W1/O). Then, the primary W1/O was poured into the 5 mL outer water (W2), which was composed of 1% PVA in water or 1% PVA in phosphate buffer (PB) at pH 8 and sonicated for another 60 s in 50% amplitude. To evaporate DCM, W1/O/W2 solution was stirred at 20 °C overnight. A-PLGA/water, A-PLGA/PB, E-PLGA/water, and E-PLGA/PB were centrifuged by $22,140 \times g$ for 30 min and washed twice with water. DPN represented the formulation of A-PLGA/PB. DPN was then resuspended in water and stored at 4 °C before use.

2.3. Preparation of iDPN and i' DP N

PEI was incorporated in DPN by adding 2 mg PEI in W1 (i) or O (i') during the primary emulsification process. Primary W1/O was then poured into 1% PVA in water or 1% PVA in pH 8 PB W2 to produce i/water-DPN, i/PB-DPN, i'/water-DPN, and i'/PB-DPN. All other processes were the same as previously mentioned.

2.4. Preparation of IDPN and AIDPN

Layer by layer (LBL) DPN was prepared by electrostatic interaction. To prepare positively charged IDPN, negatively charged DPN was added into 0.2% PEI (pH 7), incubated for 30 min, and then centrifuged by $22,140 \times g$ for 10 min twice to remove excess PEI. To

prepare negatively charged AIDPN, condensed IDPN was added dropwise into gently stirring 0.2% PAA (pH 7) for another 30 min incubation. Excess PAA was removed by $22,140 \times g$ for 10 min centrifugation. Then, the palette of nanoparticles was resuspended in water and centrifuged by $22,140 \times g$ for another 10 min.

2.5. Characterization of Nanocarriers

DPN, IDPN, and AIDPN were suspended in water, and particle size and zeta potential were measured using ZETASIZER (Malvern Nano-ZS90, Malvern, Worcestershire, UK); DPN, IDPN, and AIDPN were diluted in water to 150–200 kcps of ZETASIZER detection. Morphology of nanoparticles ($100,000 \times$ magnification) was observed by TEM (Hitachi H-700 Transmission Electron Microscope, Tokyo, Japan); nanoparticles were dropped on carbon-coated copper grids (EM RESolution, Sheffield, UK).

2.6. Encapsulation Efficiency

To determine the encapsulated efficiency percentage (EE%), nanoparticles were added to DMSO and sonicated for 10 min. After PLGA was completely dissolved in DMSO, the DOX content was measured by UV-visible spectrophotometer at 480 nm. The EE% of each formulation was calculated by the following equation:

$$EE\% = \left[\frac{\text{amount of DOX in nanoparticles}}{\text{amount of DOX initial added}} \right] * 100\% \quad (1)$$

2.7. In Vitro Release Profile of DOX from DPN, IDPN, and AIDPN

A quantity of 60 μg of DOX contained in DPN, IDPN, and AIDPN were respectively suspended in 5 mL PBS (pH 7.4 or pH 5.5, 37°C) with constant shaking at 100 rpm for 3 days. At each defined time point, nanoparticle suspensions were centrifuged at $22,140 \times g$ for 30 min and 1 mL of supernatant was replaced with PBS (pH 7.4 or pH 5.5). DOX in the supernatant was determined by the measurement of fluorescence (Ex:480/Em:550).

2.8. Cell Culture

A549, a human non-small cell lung cancer cell line (NSCLC), obtained from BCRC (Bioresource Collection and Research Center, Hsinchu, Taiwan), was grown in F-12K Medium (Kaighn's Modification of Ham's F-12 Medium) (Gibco[®], Gaithersburg, MD, USA), supplemented with 10% fetal bovine serum (FBS; Biological Industries, Cromwell, CT, USA) and 1% antibiotic-antimycotic (Gibco[®], Gaithersburg, MD, USA). A549 was incubated at 37°C in a 5% CO_2 humidified atmosphere.

2.9. Cytotoxicity

MTT assay was used to measure the cell viability after A549 was incubated with free DOX, DPN, IDPN, and AIDPN. Briefly, A549 was seeded (3500 cells/well) in 96-well plates. After overnight pre-incubation, free DOX, DPN, IDPN, and AIDPN from 0 to 1 μM were added. Cytotoxicity test in 24 h treatment, cells were incubated in a free DOX/nanoparticles-filled medium for 24 h. Then, cells were washed twice with PBS and were incubated in fresh medium for another 24 h. Cytotoxicity test in 48 h treatment, cells were incubated in a free DOX/nanoparticles-filled medium for 48 h. After incubation, the medium was then removed, and 100 μL of 5 mg/mL MTT was added and incubated for 4 h at 37°C . Finally, the supernatant was removed, and 100 μL DMSO was added to dissolved formazan. The viability of A549 was evaluated by the absorbance of 570 nm.

2.10. Cellular Uptake

The uptake of free DOX, DPN, IDPN, and AIDPN was determined using flow cytometry FACSVerse[™] (BD Biosciences, San Jose, CA, USA). A549 was seeded (10^5 cells/well) in 6-well plates at 37°C . After overnight pre-incubation, 0.1 and 1 μM of free DOX, DPN, IDPN, and AIDPN were added and incubated for another 24 h and 48 h. A549 grown in

medium without free DOX or nanoparticles was used as a control group. Then, A549 cells were washed with PBS and resuspended in 800 μ L PBS. A549 cells (10^4 cells/experiment) were analyzed by flow cytometry, and the fluorescence was detected by PE wavelength. The mean fluorescence intensity (MFI) was acquired by BD FACSuite software (BD Biosciences, San Jose, CA, USA).

2.11. Localization of Free DOX, DPN, IDPN, and AIDPN in Cells

A549 was seeded (2×10^4 cells/well) in 24-well plates and incubated overnight at 37 °C. Then, 1 μ M of free DOX, DPN, IDPN, and AIDPN was added and incubated for another 24 hr. After incubation, A549 was washed with PBS twice and stained with Hoechst 33342 and LysoTracker green DND-26. The fluorescence image of DOX, nuclei, and endo/lysosomes were obtained using a fluorescent microscope (Leica, Wetzlar, Germany).

2.12. Statistical Analysis

Data are represented as the mean \pm standard deviation (S.D.) of three repeat experiments. Student's *t*-test and one-way ANOVA with post hoc tests were used to compare experimental data, considering $p < 0.05$ as statistically significant.

3. Results

3.1. Characterization of DPN

Because DOX has high solubility in aqueous solution, the present study used double emulsion to encapsulate DOX in PLGA nanoparticles (Figure 1a) [28,29]. The EE% of two different types of PLGA (A-PLGA and E-PLGA) and two different types of W2 (water and PB; pH 8) were compared in this study. Figure 2a shows E-PLGA had a lower EE% than A-PLGA regardless of whether W2 was water or PB. In addition, W2 composed of PB increased EE% compared to water in both A-PLGA and E-PLGA. The size of all formulations was around 150 to 230 nm, and zeta potential was around -25 mV to -35 mV (Figure 2a,b). A-PLGA/PB was the best formulation due to its highest EE%. DPN for later experiments was prepared using the A-PLGA/PB formulation.

3.2. DPN Decorated with Polyelectrolytes

In addition, polycationic PEI was used to change the zeta potential of DPN to a positive value by the incorporation method (Figure 1b) [30,31] and adsorption method (Figure 1c). However, when PEI was incorporated in DPN by adding it in the W1 (iDPN) phase or the O (i'DPN) through the double emulsion process, the EE% was relatively low, regardless of whether water or PB was W2 (Figure 2c). Each of these four types of DPN incorporated by PEI exhibited a positive zeta potential (Figure 2d).

Figure 3 shows the variation of size, EE%, zeta potential, and PDI of DPN surface coated by PEI (IDPN), and then by PAA (AIDPN). After the deposition of PEI and PAA onto the core DPN surface, the particle size increased slightly and the surface charge changed from -33.77 ± 4.97 mV to 40.74 ± 1.18 mV for IDPN and -26.76 ± 2.20 mV for AIDPN, which confirmed the expected charge reversal and the opposite charge polycation/polyanion absorption. Similar to results of the incorporation method, the EE% decreased when PEI and PAA were assembled onto the DPN surface, which may be attributed to the additional washing and centrifugation steps. TEM photographs show the morphology of DPN, IDPN, and AIDPN was round (Figure 3e–g).

3.3. The Release Profile of DPN, IDPN, and AIDPN

The controlled release profile of DOX was successfully characterized by using PLGA as a carrier of nanomedicine at both pH 7.4 or pH 5.5 PBS solution (Figure 4). All three types of nanoparticles DPN, IDPN, and AIDPN at pH 5.5 had higher release rate than at pH 7.4 within three days. DPN had the highest initial release rate at both pH conditions. At pH 7.4, DOX release from AIDPN was less than that from DPN and IDPN. From the inserted graph of Figure 4, during the first eight hours at pH 7.4, there was a significant difference in the

release slope (release%/hour) between IDPN and AIDPN ($p < 0.05$). However, a significant difference between IDPN and AIDPN was not observed at pH 5.5.

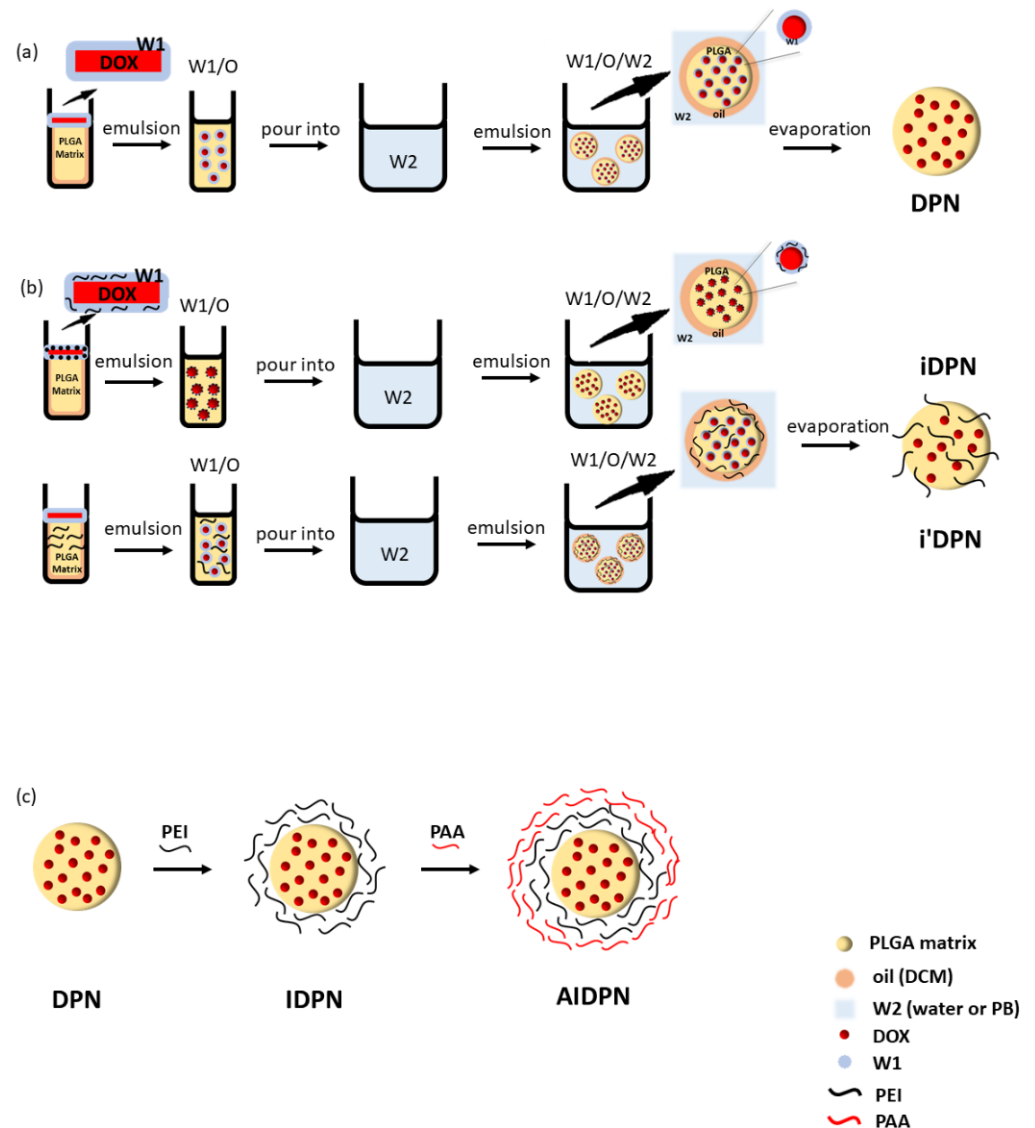


Figure 1. Schematic representation of (a) DPN (DOX-loaded PLGA nanoparticle), (b) iDPN (PEI was added in W1 during the incorporation process), i'DPN (PEI was added in O during the incorporation process), (c) IDPN (PEI-DPN), and AIDPN (PAA-PEI-DPN). Abbreviations: DCM, dichloromethane; DOX, Doxorubicin hydrochloride; W1, 0.5% DOX aqueous solution; W2, outer water, which was water or PB (phosphate buffer; pH 8); PEI, polyethylenimine; PAA, poly(acrylic acid).

3.4. Cytotoxicity

After treatment of DPN, IDPN, and AIDPN for 24 and 48 h, the viability of A549 cells decreased with increasing concentration (Figure 5). After treatment for 24 h, the difference of cytotoxicity of nanoparticles only could be observed in a 1 μM concentration. Free DOX showed the highest cytotoxicity in this study and IDPN had a significantly higher cytotoxic effect than AIDPN ($p < 0.05$). However, all three nanoparticles showed similar results after treatment for 48 h. These nanoparticles without DOX had no toxicity to A549 cells for 48 h of incubation (Figure 5c).

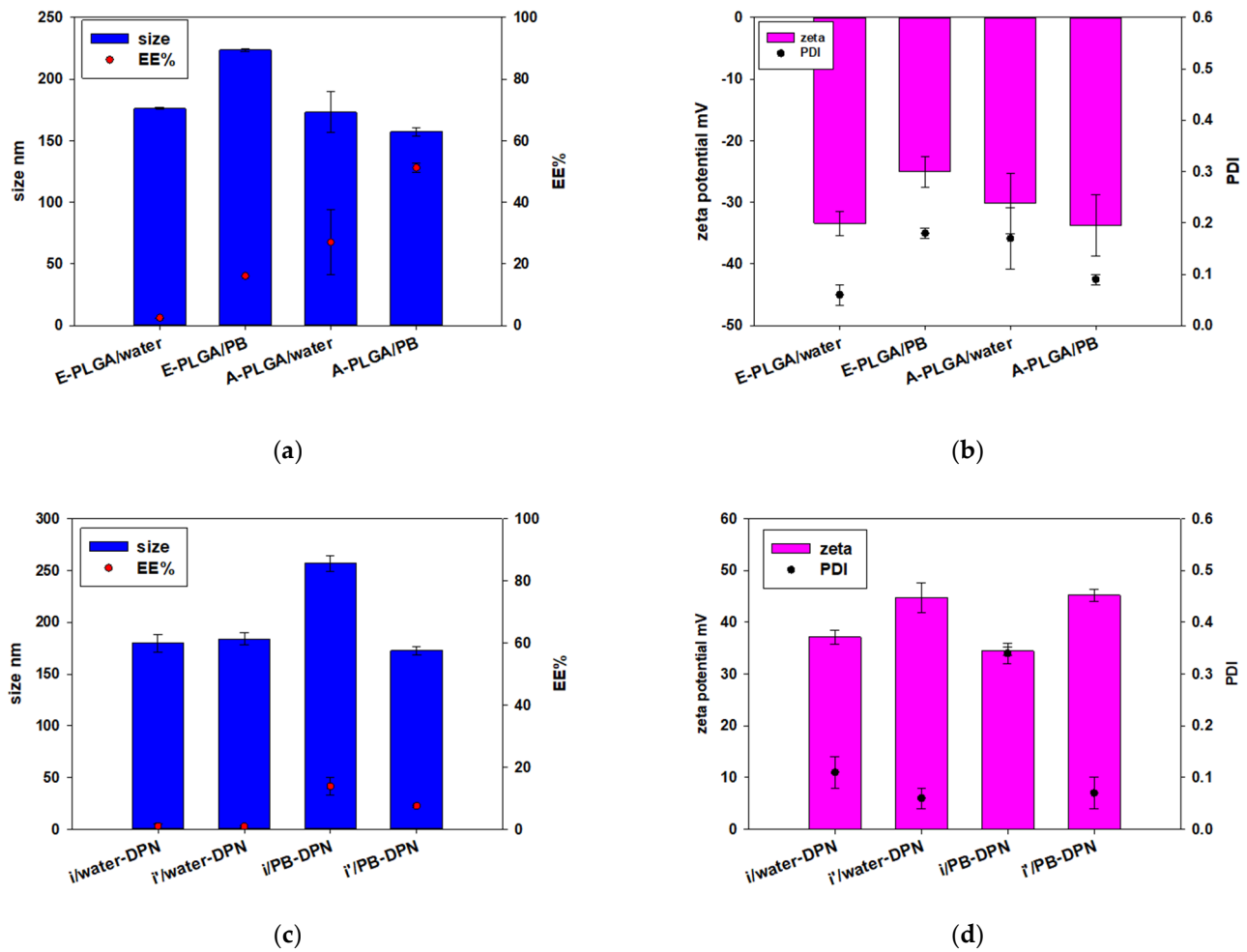


Figure 2. The effect of different types of PLGA and W2 on (a) diameter and EE% (encapsulated efficiency percentage) (b) zeta potential and PDI (polydispersity index) of DPN, and the effect of incorporated PEI and W2 on (c) diameter and EE% (d) zeta potential and PDI of iDPN and i'DPN. ($n = 3$; mean \pm standard deviation). E-PLGA/water (E-PLGA was dissolved in O and W2 was water), E-PLGA/PB (E-PLGA was dissolved in O and W2 was PB), A-PLGA/water (A-PLGA was dissolved in O and W2 was water), A-PLGA/PB (A-PLGA was dissolved in O and W2 was PB), i/water-DPN (PEI was added in W1 during the incorporation process and W2 was water), i'/water-DPN (PEI was added in O during the incorporation process and W2 was water), i/PB-DPN (PEI was added in W1 during the incorporation process and W2 was PB), i'/PB-DPN (PEI was added in O during the incorporation process and W2 was PB). Abbreviations: E-PLGA, ester terminated PLGA; A-PLGA, carboxylic acid terminated PLGA; PB, phosphate buffer (pH 8).

3.5. Cellular Uptake

Cellular uptake of free DOX, DPN, IDPN, and AIDPN was determined by the fluorescence intensity of DOX in A549 cells. Both the mean fluorescence intensity (MFI) and the number of positive cells increased with increasing nanoparticle concentration and incubation time (Figure 6). As expected, the highest uptake of IDPN nanoparticles with positive surface charge was observed in A549 cells at all incubation conditions. In contrast, although both DPN and AIDPN with negative surface charge could be taken up by A549 cells, their MFI was not higher than that of free DOX.

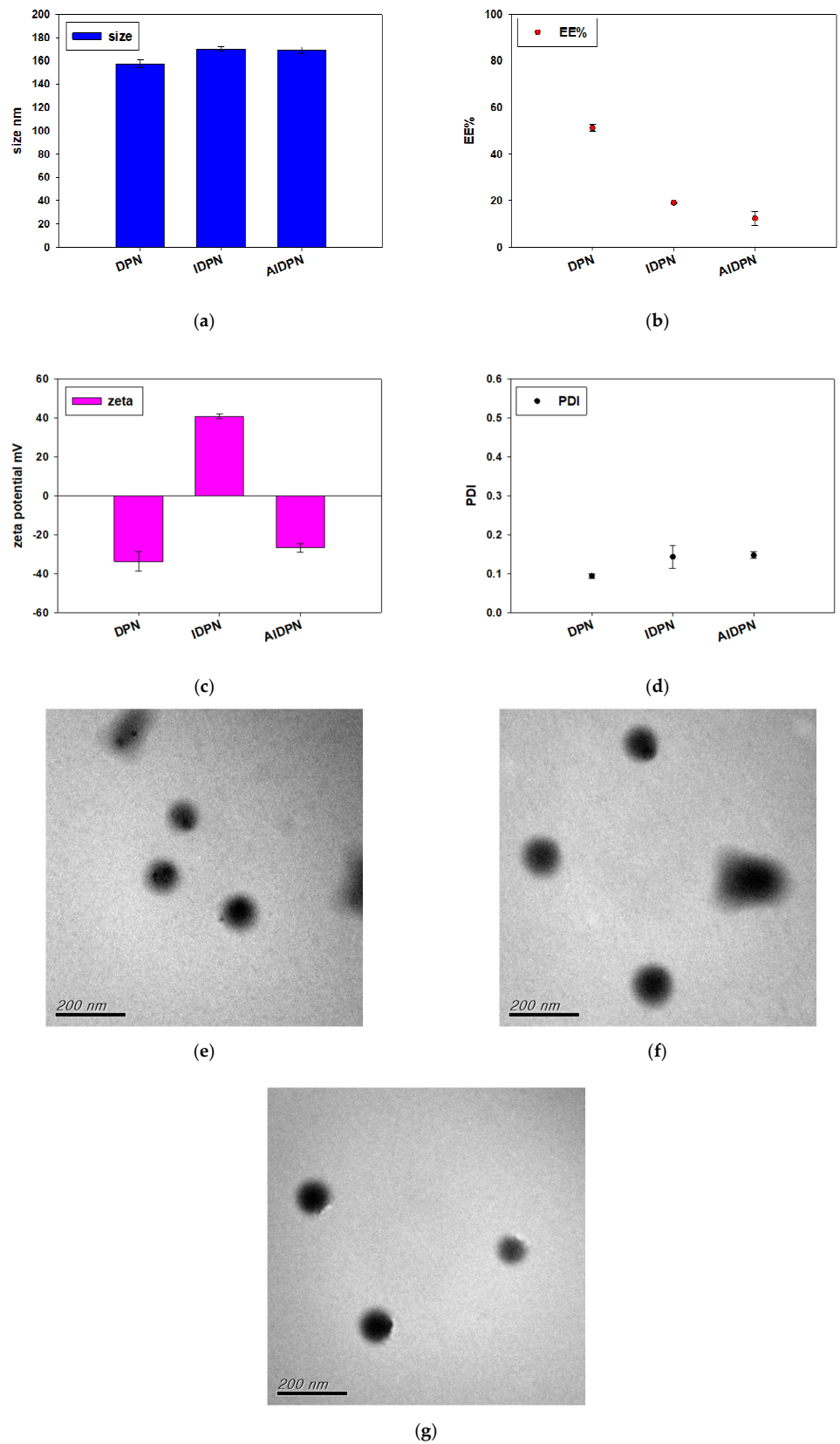


Figure 3. Characterization of DPN, IDPN, and AIDPN. (a) diameter, (b) EE%, (c) zeta potential, and (d) PDI. ($n = 3$; mean \pm standard deviation). Morphology of (e) DPN, (f) IDPN, and (g) AIDPN on TEM image.

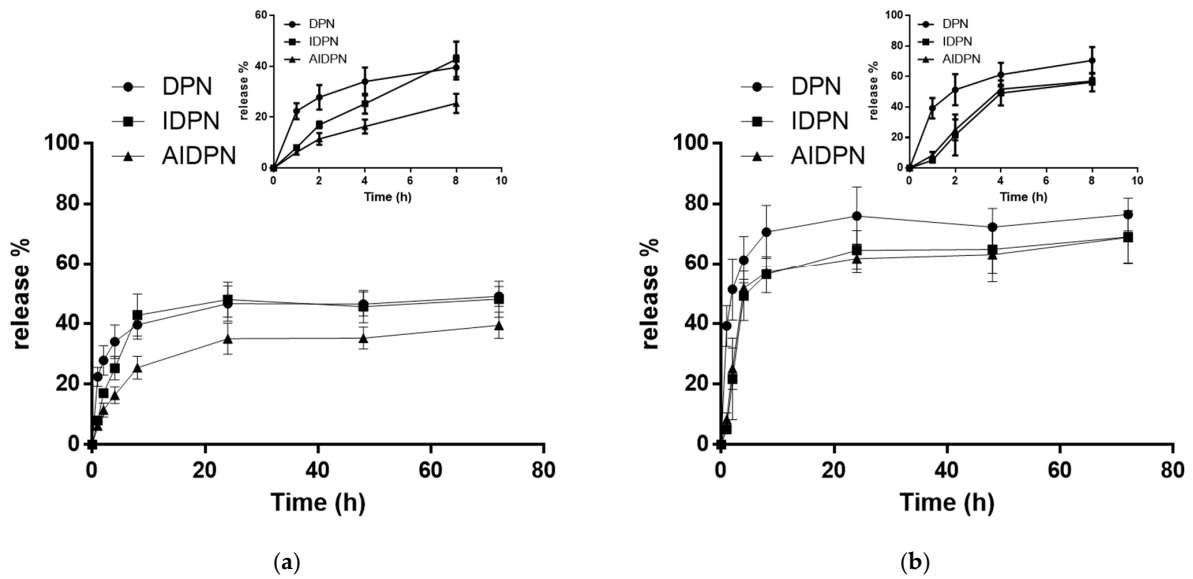


Figure 4. The release profile of DPN, IDPN, and AIDPN in (a) pH 7.4 PBS and (b) pH 5.5 PBS at 37 °C within 3 days. Inserted graphs show the release profile of DPN, IDPN, and AIDPN within 8 h in pH 7.4 PBS and pH 5.5 PBS. (n = 3; mean ± standard deviation).

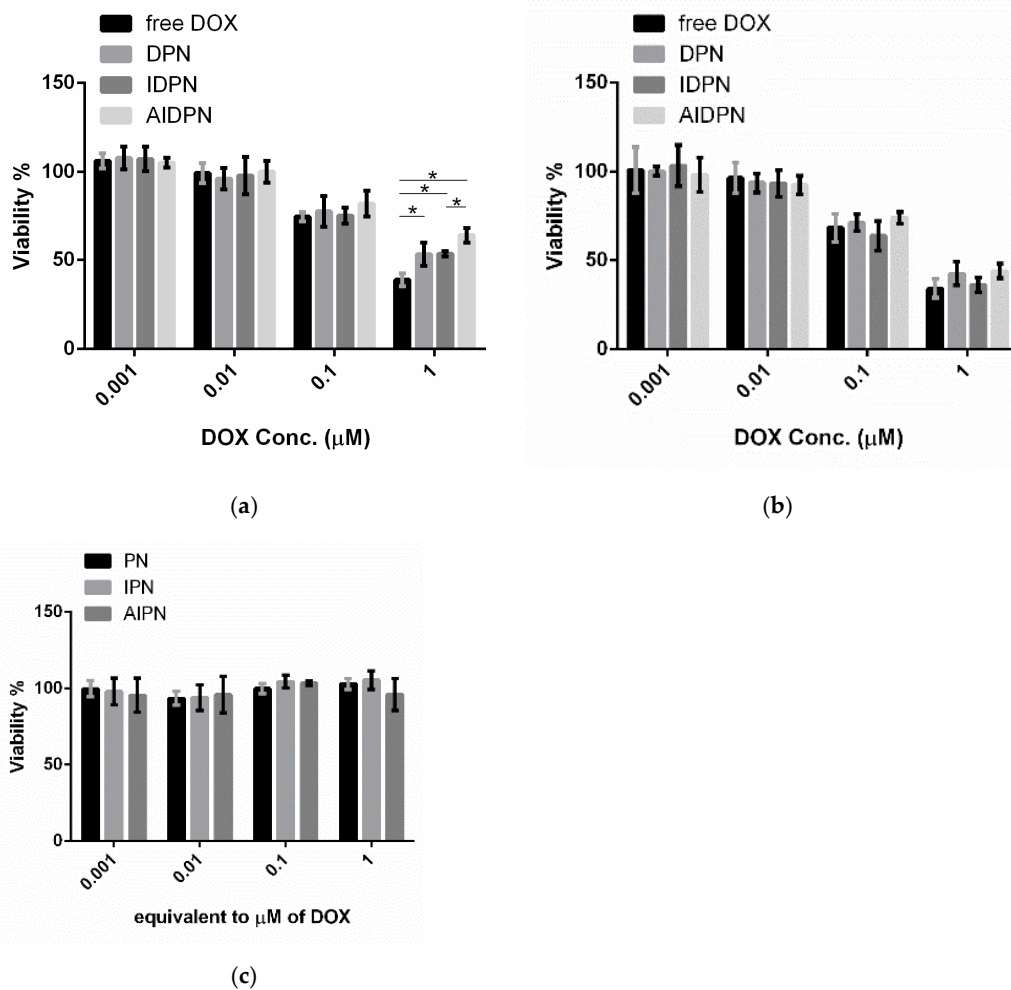


Figure 5. Cytotoxicity of free DOX, DPN, IDPN, and AIDPN with different concentrations for (a) 24 h and (b) 48 h incubation, and (c) blank nanoparticles for 48 h incubation in A549. * indicates comparison of two group, $p < 0.05$.

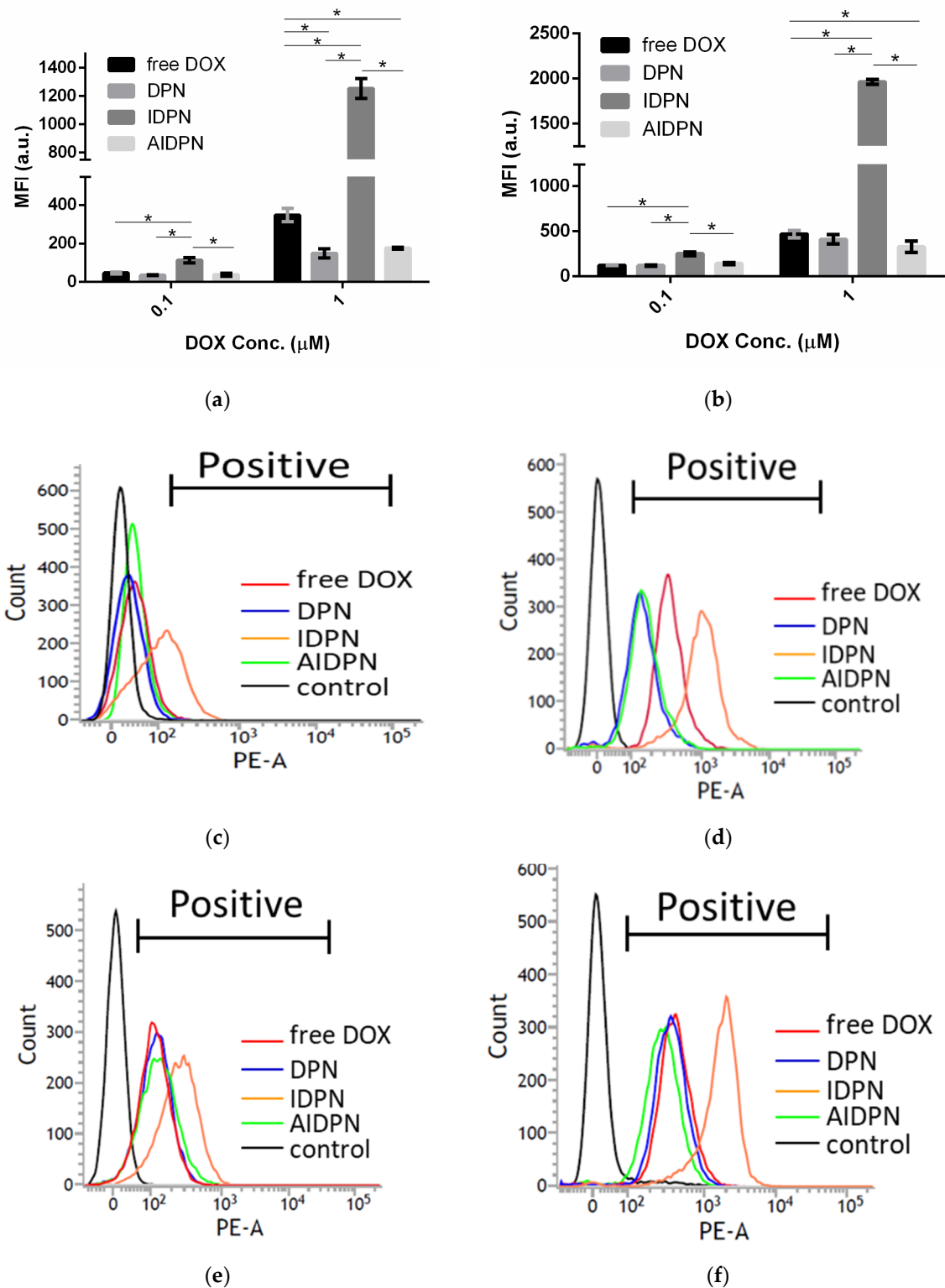


Figure 6. MFI in A549 after 0.1 and 1 μM of free DOX, DPN, IDPN and AIDPN for (a) 24 h and (b) 48 h incubation. Fluorescence intensity in A549 measured by flow cytometry after 24 h incubation of (c) 0.1 μM and (d) 1 μM of free DOX (red), DPN (blue), IDPN (orange), AIDPN (green), and control (black) and 48 h incubation of (e) 0.1 μM and (f) 1 μM of free DOX (red), DPN (blue), IDPN (orange), AIDPN (green), and control (black). Abbreviations: MFI, mean fluorescence intensity. * indicates comparison of two group, $p < 0.05$.

3.6. Endo/Lysosomes Escape Efficiency of DPN, IDPN, and AIDPN

The colocalization (yellow) of DOX (red) and Lysotracker (green) indicated that DPN, IDPN, and AIDPN were internalized in endo/lysosomes (Figure 7). IDPN was most capable of endo/lysosomal escape because it showed the greatest amount of separation of red and yellow colors. The rank of the ability of endo/lysosomal escape from high to low was IDPN, AIDPN, and DPN. Free DOX was also sequestered in acidic compartments, but it did not find that any free DOX escaped.

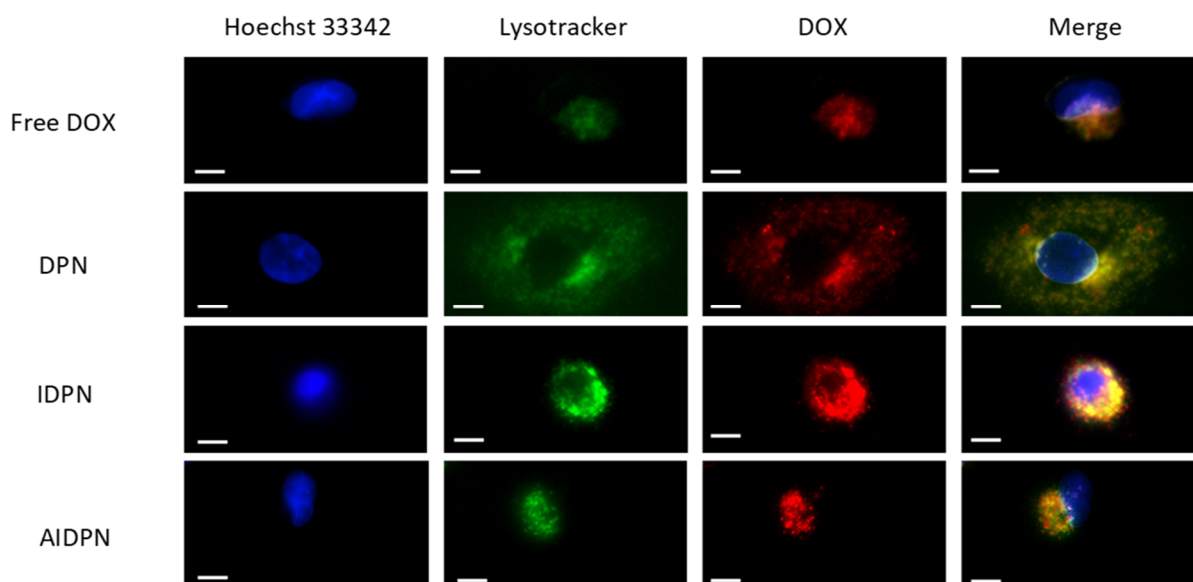


Figure 7. Fluorescence image of free DOX, DPN, IDPN, and AIDPN in A549. Blue represented nucleus (stained with Hoechst 33342); green represented endo/lysosomes (stained with Lysotracker); red was the DOX fluorescence. Scale bar 10 μm .

4. Discussion

In this study, DOX was loaded in PLGA nanoparticles for controlling release. To optimize the formulation of DPN, two types of PLGA with carboxyl and ester end groups, and two types of PVA-containing W2, water (pH 5–6), and PB (pH 7–8), were compared. According to Figure 2a, the ideal formulation was composed of A-PLGA and PB. DOX acts as a cationic ion at a pH around 4–6 and a less hydrophilic neutral compound at pH around 8.2 because the amine group pKa of DOX is 8.2 [32,33]. Therefore, the optimal formulation is probably explained by the stronger electrostatic interaction of cationic DOX and anionic A-PLGA in a weakly acidic environment, and less hydrophilic DOX is distributed to the oil phase in W2 composed of PB in a weakly basic environment during the nanoparticle formation process.

Recently, because PEI has been used in gene delivery systems due to its transfection efficiency [34,35], PEI was further added to the DPN formulation to enhance the therapeutic potency. Two procedures of PEI employed in DPN were compared in this study: (1) direct addition of PEI to nanoparticle formulation by single procedure; and (2) PEI decoration on the DPN surface using the electrostatic absorption process. However, positively charged PEI could occupy the carboxylic acid of A-PLGA, so both A-PLGA and E-PLGA had low efficiency to encapsulate DOX in this situation (Figure 2c). Therefore, the DPN surface was decorated through an additional layer of PEI. In addition, PAA, pH-dependent anionic polyelectrolyte, has been used to prepare a pH-responsive drug delivery system [36,37]. To prepare DOX-loaded nanoparticles with both endo/lysosomal escape and pH sensitive property, the present study tried to decorate PEI and PAA on DPN using the LBL self-assembly technique.

During the LBL self-assembly process, the pH value of polyelectrolyte solutions should be considered. The ionization degree of PAA was increased with the increasing pH value, and the protonated degree of PEI could be enhanced with the decreasing pH value [38,39]. Furthermore, both alkaline and acid surroundings accelerated the degradation of PLGA [40]. Due to all of these restrictions, the process of LBL self-assembly should be applied using a solution of around pH 7.

Due to the penetration of water in nanoparticles enhanced by the high content of water-soluble drugs [41], hydrophilic DOX in DPN might facilitate PBS penetration into DPN. DOX was then transported into the water-filled pore network and diffused into the medium. Again, because acid surrounding could increase the solubility of cationic DOX, the amount of DOX in pores would increase when DPN was suspended in pH 5.5 PBS. As a result, all DPN, IDPN, and AIDPN had a higher release percentage at pH 5.5 PBS than at pH 7.4 PBS (Figure 4). Generally, the environment surrounded tumor tissue is slightly acidic than physiological conditions. This release profile implied that the acidic condition can promote DOX released from DPN, IDPN, and AIDPN, with the potential for selective tumor therapy. In particular, DOX release of AIDPN at pH 5.5 continued to constantly increase within the 72 h of the experiment until it reached its equilibrium at 63.9%, showing a significantly higher drug release (39.4%) than the corresponding nanoparticles in the physiological solution (pH 7.4). The increased DOX release at pH = 5.5 can be attributed to the higher anionic degree of PAA at pH 7.4 than at pH 5.5 [38,39] with stronger binding affinity to protonated DOX, which resulted in an approximately 1.6 times higher drug release from AIDPN at pH = 5.5 compared to that at pH = 7.4. Due to the additional PAA layer, the release profile of IDPN and AIDPN was significantly different in pH 7.4 PBS but similar in pH 5.5 PBS (Figure 4). Therefore, AIDPN can be considered the best option in this study with the lowest DOX release from nanoparticles to reduce the side effect on normal cells under physiological conditions.

Previous research has demonstrated that the uptake of nanoparticles with a positive surface charge was higher than that with a negative surface charge in cancer cells [42]. Similarly, IDPN had significantly higher efficiency than DPN and AIDPN in cellular uptake (Figure 6). However, compared to that of DPN, the higher uptake of IDPN by A549 cells did not correspond with the higher cytotoxicity at 1 μ M concentration (Figure 5), which may be due to the more DOX release from DPN within the initial four hours (Figure 4). This indicates the burst effect of DPN could be shielded by the PEI layer on the outside surface. Additionally, the PAA layer on the IDPN surface further shielded the AIDPN, possibly contributing to low release and cytotoxicity.

The endo/lysosomal escape of drug is considered to affect the efficiency of drug cytotoxicity strongly [43]. IDPN was shown to be the most efficient endo/lysosomes escape in three different types of nanoparticles (Figure 7). This implied that IDPN was entrapped in cells by endocytosis and would be delivered to cytoplasm rather than degraded in acidic endo/lysosomes or ejected by lysosome secretion [44,45]. The escape ability of IDPN could be attributed to PEI, whose buffer capacity was supposed to rupture acid organelles by the "proton sponge" effect [19–22]. PAA seemed to diminish the escape ability contributed from PEI due to fewer red spots spread from the yellow region when A549 was incubated with AIDPN. However, compared to DPN, AIDPN, with the outermost negatively charged PAA layer, still retained better endo/lysosomal escape ability. Therefore, the cationic/anionic LBL controlled release nanoparticle, AIDPN, is an ideal formulation in cancer therapy for its pH-dependent release profile and endo/lysosomal escape ability. In further investigation, we will deliver AIDPN to animal model to evaluate safety, efficacy, and pharmacokinetics in vivo. Furthermore, we plan to prepare a lyophilized formulation of AIDPN to dissolve the problem of not-convenient for commercial application.

5. Conclusions

In summary, based on the optimized formulation of A-PLGA and the W2 phase, three types of nanoparticles—DPN, IDPN, and AIDPN—were prepared using the PEI/PAA

LBL technique. DPN showed poor ability in terms of endo/lysosomal escape, and its undesired high burst release in physiological conditions might result in greater toxicity in normal cells. IDPN decorated with PEI, compared to DPN, had a slower release rate in physiological conditions but had higher efficiency in cellular uptake and endo/lysosomal escape. However, the cationic surface of IDPN might restrict its application in vivo due to aggregation with serum protein. AIDPN, with the outermost negatively charged PAA layer, retained endo/lysosomal escape ability and mitigated the risk of aggregation with serum protein in vivo. In addition, the pH-sensitive PAA modified AIDPN to possess the best pH-dependent release profile. As a result, AIDPN, with the properties of both PEI and PAA, was found to be the most suitable cancer therapy amount these three different nanoparticles.

Author Contributions: Conceptualization, L.-H.T. and T.-H.Y.; methodology, L.-H.T., C.-H.Y., H.-Y.H., and T.-H.Y.; data acquisition, L.-H.T., C.-H.Y., and H.-Y.H.; data analysis and interpretation, L.-H.T. and T.-H.Y.; visualization, L.-H.T. and T.-H.Y.; writing—original draft preparation, L.-H.T. and T.-H.Y.; writing—review and editing, L.-H.T. and T.-H.Y.; supervision, T.-H.Y.; project administration, T.-H.Y. All authors have read and agreed to the published version of the manuscript.

Funding: This research was funded by the Ministry of Education and Ministry of Science and Technology (108-2314-B-002 -104 -MY3), Taiwan.

Institutional Review Board Statement: Not applicable.

Informed Consent Statement: Not applicable.

Data Availability Statement: Not applicable.

Acknowledgments: We thank the department of electron microscopy, School of Science, Taiwan University, Ya-Yun Yang and Ching-Yen Lin.

Conflicts of Interest: The authors declare no conflict of interest.

Abbreviations

DPN	DOX-loaded PLGA nanoparticle
iDPN	PEI was added in W1 during the incorporation process
i'DPN	PEI was added in O during the incorporation process
IDPN	PEI-DPN
AIDPN	PAA-PEI-DPN

References

1. Saratale, R.G.; Karuppusamy, I.; Saratale, G.D.; Pugazhendhi, A.; Kumar, G.; Park, Y.; Ghodake, G.S.; Bharagava, R.N.; Banu, J.R.; Shin, H.S. A comprehensive review on green nanomaterials using biological systems: Recent perception and their future applications. *Colloids Surfaces B Biointerfaces* **2018**, *170*, 20–35. [[CrossRef](#)]
2. Peer, D.; Karp, J.M.; Hong, S.; Farokhzad, O.C.; Margalit, R.; Langer, R. Nanocarriers as an emerging platform for cancer therapy. *Nat. Nanotechnol.* **2007**, *2*, 751–760. [[CrossRef](#)] [[PubMed](#)]
3. Rosenblum, D.; Joshi, N.; Tao, W.; Karp, J.M.; Peer, D. Progress and challenges towards targeted delivery of cancer therapeutics. *Nat. Commun.* **2018**, *9*, 1–12. [[CrossRef](#)]
4. Rizvi, S.A.; Saleh, A.M. Applications of nanoparticle systems in drug delivery technology. *Saudi Pharm. J.* **2018**, *26*, 64–70. [[CrossRef](#)]
5. Patra, J.K.; Das, G.; Fraceto, L.F.; Campos, E.V.R.; del Pilar Rodriguez-Torres, M.; Acosta-Torres, L.S.; Diaz-Torres, L.A.; Grillo, R.; Swamy, M.K.; Sharma, S.; et al. Nano based drug delivery systems: Recent developments and future prospects. *J. Nanobiotechnol.* **2018**, *16*, 71. [[CrossRef](#)] [[PubMed](#)]
6. Saratale, R.G.; Cho, S.-K.; Saratale, G.D.; Kadam, A.A.; Ghodake, G.S.; Kumar, M.; Bharagava, R.N.; Kumar, G.; Kim, D.S.; Mulla, S.I.; et al. A comprehensive overview and recent advances on polyhydroxyalkanoates (PHA) production using various organic waste streams. *Bioresour. Technol.* **2021**, *325*, 124685. [[CrossRef](#)] [[PubMed](#)]
7. Karlsson, J.; Vaughan, H.J.; Green, J.J. Biodegradable Polymeric Nanoparticles for Therapeutic Cancer Treatments. *Annu. Rev. Chem. Biomol. Eng.* **2018**, *9*, 105–127. [[CrossRef](#)]
8. Su, S.; Kang, P.M. Systemic Review of Biodegradable Nanomaterials in Nanomedicine. *Nanomaterials* **2020**, *10*, 656. [[CrossRef](#)]

9. Blasi, P. Poly(lactic acid)/poly(lactic-co-glycolic acid)-based microparticles: An overview. *J. Pharm. Investig.* **2019**, *49*, 337–346. [[CrossRef](#)]
10. Chereddy, K.K.; Vandermeulen, G.; Pr at, V. PLGA based drug delivery systems: Promising carriers for wound healing activity. *Wound Repair Regen.* **2016**, *24*, 223–236. [[CrossRef](#)]
11. Sah, E.; Sah, H. Recent Trends in Preparation of Poly(lactide-co-glycolide) Nanoparticles by Mixing Polymeric Organic Solution with Antisolvent. *J. Nanomater.* **2015**, *2015*, 794601. [[CrossRef](#)]
12. Rezvantalab, S.; Drude, N.I.; Moraveji, M.K.; G vener, N.; Koons, E.K.; Shi, Y.; Lammers, T.; Kiessling, F. PLGA-Based Nanoparticles in Cancer Treatment. *Front. Pharmacol.* **2018**, *9*, 1260. [[CrossRef](#)] [[PubMed](#)]
13. Thorn, C.F.; Oshiro, C.; Marsh, S.; Hernandez-Boussard, T.; McLeod, H.; Klein, T.E.; Altman, R.B. Doxorubicin pathways: Pharmacodynamics and adverse effects. *Pharm. Genom.* **2011**, *21*, 440–446. [[CrossRef](#)]
14. Mizutani, H.; Tada-Oikawa, S.; Hiraku, Y.; Kojima, M.; Kawanishi, S. Mechanism of apoptosis induced by doxorubicin through the generation of hydro-gen peroxide. *Life Sci.* **2005**, *76*, 1439–1453. [[CrossRef](#)]
15. Zhao, L.; Zhang, B. Doxorubicin induces cardiotoxicity through upregulation of death receptors mediated apoptosis in cardiomyocytes. *Sci. Rep.* **2017**, *7*, srep44735. [[CrossRef](#)] [[PubMed](#)]
16. Rochette, L.; Guenancia, C.; Gudjoncik, A.; Hachet, O.; Zeller, M.; Cottin, Y.; Vergely, C. Anthracyclines/trastuzumab: New aspects of cardiotoxicity and molecular mechanisms. *Trends Pharmacol. Sci.* **2015**, *36*, 326–348. [[CrossRef](#)]
17. Yan, L.; Shen, J.; Wang, J.; Yang, X.; Dong, S.; Lu, S. Nanoparticle-Based Drug Delivery System: A Patient-Friendly Chemotherapy for Oncology. *Dose-Response* **2020**, *18*, 1559325820936161. [[CrossRef](#)] [[PubMed](#)]
18. Zhao, C.-Y.; Cheng, R.; Yang, Z.; Tian, Z.-M. Nanotechnology for Cancer Therapy Based on Chemotherapy. *Molecules* **2018**, *23*, 826. [[CrossRef](#)] [[PubMed](#)]
19. Benjaminsen, R.V.; Mattebjerg, M.A.; Henriksen, J.R.; Moghimi, S.M.; Andresen, T.L. The possible “proton sponge” effect of polyethylenimine (PEI) does not include change in lysosomal pH. *Mol. Ther.* **2013**, *21*, 149–157. [[CrossRef](#)] [[PubMed](#)]
20. Insua, I.; Wilkinson, A.; Fernandez-Trillo, F. Polyion complex (PIC) particles: Preparation and biomedical applications. *Eur. Polym. J.* **2016**, *81*, 198–215. [[CrossRef](#)] [[PubMed](#)]
21. Fortuni, B.; Inose, T.; Ricci, M.; Fujita, Y.; Van Zundert, I.; Masuhara, A.; Fron, E.; Mizuno, H.; Latterini, L.; Rocha, S.; et al. Polymeric Engineering of Nanoparticles for Highly Efficient Multifunctional Drug Delivery Systems. *Sci. Rep.* **2019**, *9*, 2666. [[CrossRef](#)]
22. Bus, T.; Traeger, A.; Schubert, U.S. The great escape: How cationic polyplexes overcome the endosomal barrier. *J. Mater. Chem. B* **2018**, *6*, 6904–6918. [[CrossRef](#)]
23. Nuhn, L.; Gietzen, S.; Mohr, K.; Fischer, K.; Toh, K.; Miyata, K.; Matsumoto, Y.; Kataoka, K.; Schmidt, M.; Zentel, R. Aggregation Behavior of Cationic Nanohydrogel Particles in Human Blood Serum. *Biomacromolecules* **2014**, *15*, 1526–1533. [[CrossRef](#)] [[PubMed](#)]
24. Brunot, C.; Ponsonnet, L.; Lagneau, C.; Farge, P.; Picart, C.; Grosogeat, B. Cytotoxicity of polyethylenimine (PEI), precursor base layer of polyelectrolyte multilayer films. *Biomater.* **2007**, *28*, 632–640. [[CrossRef](#)] [[PubMed](#)]
25. Zhou, J.; Moya, S.; Ma, L.; Gao, C.; Shen, J. Polyelectrolyte Coated PLGA Nanoparticles: Templatation and Release Behavior. *Macromol. Biosci.* **2009**, *9*, 326–335. [[CrossRef](#)]
26. Sung, H.; Ferlay, J.; Siegel, R.L.; Laversanne, M.; Soerjomataram, I.; Jemal, A.; Bray, F. Global cancer statistics 2020: GLOBOCAN estimates of incidence and mortality worldwide for 36 cancers in 185 countries. *CA A Cancer J. Clin.* **2021**. [[CrossRef](#)]
27. Molina, J.R.; Yang, P.; Cassivi, S.D.; Schild, S.E.; Adjei, A.A. Non-small cell lung cancer: Epidemiology, risk factors, treatment, and survivorship. *Mayo Clin. Proc.* **2008**, *83*, 584–594. [[CrossRef](#)]
28. Babos, G.; Bir o, E.; Meiczinger, M.; Feczko, T. Dual Drug Delivery of Sorafenib and Doxorubicin from PLGA and PEG-PLGA Polymeric Nanoparticles. *Polymers* **2018**, *10*, 895. [[CrossRef](#)] [[PubMed](#)]
29. Mosafer, J.; Teymouri, M. Comparative study of superparamagnetic iron oxide/doxorubicin co-loaded poly (lactic-co-glycolic acid) nanospheres prepared by different emulsion solvent evaporation methods. *Artif. Cells Nanomed. Biotechnol.* **2018**, *46*, 1146–1155. [[CrossRef](#)] [[PubMed](#)]
30. Sharifnia, Z.; Bandehpour, M.; Hamishehkar, H.; Mosaffa, N.; Kazemi, B.; Zarghami, N. In-vitro Transcribed mRNA Delivery Using PLGA/PEI Nanoparticles into Human Monocyte-derived Dendritic Cells. *Iranian J. Pharm. Res. IJPR* **2019**, *18*, 1659–1675.
31. Katas, H.; Cevher, E.; Alpar, H.O. Preparation of polyethylenimine incorporated poly(D,L-lactide-co-glycolide) nanoparticles by spontaneous emulsion diffusion method for small interfering RNA delivery. *Int. J. Pharm.* **2009**, *369*, 144–154. [[CrossRef](#)]
32. Tewes, F.; Munnier, E.; Antoon, B.; Okassa, L.N.; Cohen-Jonathan, S.; Marchais, H.; Douziech-Eyrolles, L.; Souc e, M.; Dubois, P.; Chourpa, I. Comparative study of doxorubicin-loaded poly(lactide-co-glycolide) nanoparticles prepared by single and double emulsion methods. *Eur. J. Pharm. Biopharm.* **2007**, *66*, 488–492. [[CrossRef](#)] [[PubMed](#)]
33. F l p, Z.; Gref, R.; Loftsson, T. A permeation method for detection of self-aggregation of doxorubicin in aqueous environment. *Int. J. Pharm.* **2013**, *454*, 559–561. [[CrossRef](#)]
34. Zakeri, A.; Kouhbanani, M.A.J.; Beheshtkhoo, N.; Beigi, V.; Mousavi, S.M.; Hashemi, S.A.R.; Zade, A.K.; Amani, A.M.; Savardash-taki, A.; Mirzaei, E.; et al. Polyethylenimine-based nanocarriers in co-delivery of drug and gene: A developing horizon. *Nano Rev. Exp.* **2018**, *9*, 1488497. [[CrossRef](#)] [[PubMed](#)]
35. Sung, Y.K.; Kim, S.W. Recent advances in polymeric drug delivery systems. *Biomater. Res.* **2020**, *24*, 12. [[CrossRef](#)] [[PubMed](#)]
36. Pal, A.; Bajpai, J.; Bajpai, A.K. Poly (acrylic acid) grafted gelatin nanocarriers as swelling controlled drug delivery system for op-timized release of paclitaxel from modified gelatin. *J. Drug Deliv. Sci. Technol.* **2018**, *45*, 323–333. [[CrossRef](#)]

37. Song, Q.; Jia, J.; Niu, X.; Zheng, C.; Zhao, H.; Sun, L.; Zhang, H.; Wang, L.; Zhang, Z.; Zhang, Y. An oral drug delivery system with programmed drug release and imaging properties for orthotopic colon cancer therapy. *Nanoscale* **2019**, *11*, 15958–15970. [[CrossRef](#)]
38. Häuser, M.; Langer, K.; Schönhoff, M. pH-Triggered release from surface-modified poly(lactic-co-glycolic acid) nanoparticles. *Beilstein J. Nanotechnol.* **2015**, *6*, 2504–2512. [[CrossRef](#)] [[PubMed](#)]
39. Yuan, W.; Li, C.M. Exponentially growing layer-by-layer assembly to fabricate pH-responsive hierarchical nanoporous polymeric film and its superior controlled release performance. *Chem. Commun.* **2010**, *46*, 9161–9163. [[CrossRef](#)] [[PubMed](#)]
40. Makadia, H.K.; Siegel, S.J. Poly Lactic-co-Glycolic Acid (PLGA) as Biodegradable Controlled Drug Delivery Carrier. *Polymers* **2011**, *3*, 1377–1397. [[CrossRef](#)] [[PubMed](#)]
41. Han, F.Y.; Thurecht, K.J.; Whittaker, A.K.; Smith, M.T. Bioerodable PLGA-Based Microparticles for Producing Sustained-Release Drug Formulations and Strategies for Improving Drug Loading. *Front. Pharmacol.* **2016**, *7*, 185. [[CrossRef](#)] [[PubMed](#)]
42. Jeon, S.; Clavadetscher, J.; Lee, D.-K.; Chankeshwara, S.V.; Bradley, M.; Cho, W.-S. Surface Charge-Dependent Cellular Uptake of Polystyrene Nanoparticles. *Nanomaterials* **2018**, *8*, 1028. [[CrossRef](#)] [[PubMed](#)]
43. Plaza-Ga, I.; Manzaneda-González, V.; Kisovec, M.; Almendro-Vedia, V.; Muñoz-Úbeda, M.; Anderluh, G.; Guerrero-Martínez, A.; Natale, P.; Montero, I.L. pH-triggered endosomal escape of pore-forming Listeriolysin O toxin-coated gold nanoparticles. *J. Nanobiotechnol.* **2019**, *17*, 108. [[CrossRef](#)] [[PubMed](#)]
44. Zeng, J.; Martin, A.; Han, X.; Shirihai, O.S.; Grinstaff, M.W. Biodegradable PLGA Nanoparticles Restore Lysosomal Acidity and Protect Neural PC-12 Cells against Mitochondrial Toxicity. *Ind. Eng. Chem. Res.* **2019**, *58*, 13910–13917. [[CrossRef](#)]
45. Park, J.H.; Oh, N. Endocytosis and exocytosis of nanoparticles in mammalian cells. *Int. J. Nanomed.* **2014**, *1*, 51. [[CrossRef](#)] [[PubMed](#)]